Molecular Dynamics Investigation of Dipeptide - Transition Metal Salts in Aqueous Solutions

M. S. Santosh,[†] Alexander P. Lyubartsev,*[,‡] Alexander A. Mirzoev,[‡] and D. Krishna Bhat[†]

Physical Chemistry Division, Department of Chemistry, National Institute of Technology Karnataka, Surathkal, Mangalore-575025, India, and Division of Physical Chemistry, Department of Materials and Environmental Chemistry, Arrhenius Laboratory, Stockholm University, S-10691, Stockholm, Sweden

Received: September 2, 2010; Revised Manuscript Received: October 28, 2010

Molecular dynamics (MD) simulations of glycylglycine dipeptide with transition metal ions (Mn^{2+}, Fe^{2+}, Co^{2+}, Ni^{2+}, Cu^{2+}, and Zn^{2+}) in aqueous solutions have been carried out to get an insight into the solvation structure, intermolecular interactions, and salt effects in these systems. The solvation structure and hydrogen bonding were described in terms of radial distribution function (RDF) and spatial distribution function (SDF). The dynamical properties of the solvation structure were also analyzed in terms of diffusion and residence times. The simulation results show the presence of a well-defined first hydration shell around the dipeptide, with water molecules forming hydrogen bonds to the polar groups of the dipeptide. This shell is, however, affected by the strong electric field of divalent metal ions, which at higher ion concentrations lead to the shift in the dipeptide−water RDFs. Higher salt concentrations lead also to increased residence times and slower diffusion rates. In general, smaller ions (Cu^{2+}, Zn^{2+}) demonstrate stronger binding to dipeptide than the larger ones (Fe^{2+}, Mn^{2+}). Simulations do not show any stronger association of peptide molecules indicating their dissolution in water. The above results may be of potential interest to future researchers on these molecular interactions.

1. Introduction

The interactions of proteins with their surrounding environment play an important role in their conformational characteristics and thus in their biological function.[1,2] The stability of protein depends sensitively on thermodynamic conditions such as solvent, temperature, pressure, and coexisting solutes. To get a better understanding of the role of water in the fundamental aspects of biomolecular stability and structural integrity, a microscopic description of the hydration of biological molecules as well as the bulk water structure present around biomolecules is very much necessary. Theoretical modeling of these interactions aiming at a comprehensive view of cause and effect has always been a tremendous challenge.[3] Among various thermodynamics conditions such as temperature, pressure, substrate, and solvent, the most extensively studied are the salt effects.[4−6] Salt-induced electrostatic forces are known to play a vital role in modifying the properties of proteins like solubility and denaturation, due to the presence of charged groups at the surface of proteins.[7,8] In biological and medical fields, the function of divalent cations is very significant. For instance, metal ions such as Mn^{2+} and Zn^{2+} are essential factors for many enzymatic reactions. Owing to their special electronic properties and ability to exist in more than one oxidation state, Cu^{2+} and Fe^{2+} are key components of respiration and photosynthesis.[9−14] It is a well-known fact that the effect of various ions on the local water structure differ widely.[15−19] For a quantitative description of physical and chemical phenomena of metal solvation, molecular dynamics (MD) simulations have proven to be a suitable alternative.[20] Although the structural, dynamical, and other properties of peptides and metal salts in aqueous solutions have been a subject of a number of previous research,[21−26] MD studies involving peptides and transition metal salts in aqueous solutions are limited. Given the importance of divalent metal ions in biological systems, it seems interesting to investigate how these highly charged ions affect hydration properties of peptides and their interactions. Also, recent development in the area of statistical theories of solute−solute and solute−solvent models of liquid state and discussions on preferential solvation mechanisms[26] generated curiosity in us to study the molecular interactions occurring in the above systems. Molecular dynamics simulations are capable of providing detailed information on various types of interactions at the nanosecond time-scale aiding further investigation of this problem.

Thus, to gain a better view of how different divalent metal ions interact with simplest peptide, glycylglycine (GG) in water solution, a comprehensive set of molecular dynamics simulation has been carried out to analyze the connection between molecular interactions and structural properties of the solute−solvent system. It may be instructive to start with the smallest and simplest peptide molecule before moving on to the complex one. Furthermore, in this paper, the effects of six different transition metal ions (Mn^{2+}, Fe^{2+}, Co^{2+}, Ni^{2+}, Cu^{2+}, and Zn^{2+}) on glycylglycine hydration and molecular association are quantitatively described from an analysis of the MD simulation trajectories. In addition, the above studies also give scope for further research on the structure and dynamics of various biomolecules in diverse environments.

2. Computational Methods

The structure of dipeptide glycylglycine is shown in Figure 1. We describe it using the all-atom AMBER force field (version 4.1 from 1995), specially refined for protein simulations.[27] Partial

* Corresponding author. E-mail: alexander.lyubartsev@mmk.su.se.
[†] National Institute of Technology Karnataka.
[‡] Stockholm University.

10.1021/jp108376j
Published on Web 11/18/2010

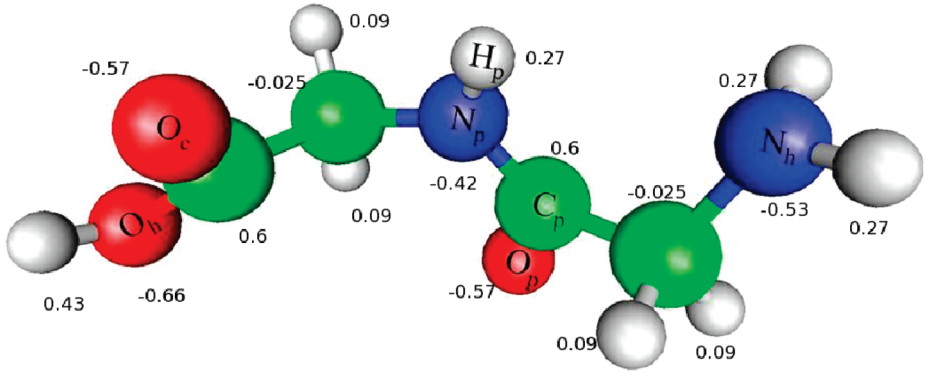

Figure 1. Structure of glycylglycine, with atom names referred in the text and partial charges.

TABLE 1: Lennard-Jones Potential $U(r) = 4\varepsilon((\sigma/r)^{12} - (\sigma/r)^6)$ Parameters for the Ions Studied

ion	σ/Å	ε/kJ·mol^{-1}
Mn^{2+}	2.5914	0.1256
Fe^{2+}	2.4032	0.1105
Co^{2+}	2.1857	0.1197
Zn^{2+}	2.0471	0.1360
Ni^{2+}	1.9494	0.1532
Cu^{2+}	1.8405	0.1787
Cl^-	4.8600	0.17

atom charges were parametrized by electrostatic potential fitting from Hartree−Fock (6-31G*) computations of the optimized GG geometry, performed by the Gaussian-03 package. As a water model, we use the flexible SPC water by Toukan and Rahman.[28] Ions were described by a combination of Lennard-Jones and electrostatic interactions. For divalent ions we used Lennard-Jones parameters, derived from the data on hydration free energies and diffraction structures by Babu and Lim[29] (applying conversion $\sigma = 2^{-1/6}R_{min}$ to the data of Table 5 of that work). Cl^- anion was described by the Heinzinger parameter set.[30] For convenience of the reader, the Lennard-Jones parameters of ions used in this work are summarized in Table 1.

All the MD simulations were carried out using the general purpose simulation package MDynaMix.[31] The double-time step method by Tuckerman et al.[32] was applied with 0.2 fs time step to describe the fast motional modes, such as bond stretching, angular and torsional bending. Even the short-range nonbonded interactions within 5 Å distance were treated with the faster time step. The long-distance nonbonded interactions were integrated after each 2.0 fs. Ewald summation[33] was used to treat the long-range Coulombic interactions. The cutoff distance in the real space, R_{cut}, was optimized for a maximum computational performance and was equal to $R_{cut} = 11.0$ Å, and the Ewald parameter α was taken as $2.8/R_{cut}$. Simulations were carried out in an *NPT* ensemble using periodic boundaries. The coupling of temperature and pressure bath was established by means of Nose−Hoover thermobarostat,[34] with relaxation times of 30 and 700 fs for the temperature and pressure fluctuations, respectively.

The number of various molecular species in different systems is listed in Table 2. Briefly, system I includes a single GG dipeptide, single cation, and two chloride anions; system II corresponds to a higher ion concentration while system III represents a higher dipeptide concentration. During the first 0.2 ns of simulation, glycylglycine was kept fixed, allowing the equilibration of water molecules and ions in the system. The system was further equilibrated during the next 0.3 ns of simulation where all the atoms in glycylglycine were allowed to move. Then, the production runs were carried out for further

TABLE 2: Number of Molecules/Ions in Three Different Systems Studied

System	H_2O	glycylglycine	metal Ion (Mn, Fe, Co, Ni, Cu, or Zn)	chloride ion
I	500	1	1	2
II	500	2	5	10
III	500	5	1	2

9.5 ns, leading to a total simulation length of 10 ns. The temperature was kept constant at 298.15 K and pressure at 1 atm during all simulations.

The radial distribution function (RDF) is traditionally used to analyze solution structure revealed from either experimental or computer simulation studies. The RDF function $g_{ij}(r)$ describes the relative probability of finding a pair of atoms i and j at a distance r apart compared to a completely random distribution at the same density.[35] The appropriately normalized running integral of the RDF gives the number of atoms j (and hence the number of molecules they belong to) in a sphere of radius r around the atom i, which can be used to define the coordination number (traditionally by the position of the first RDF minimum). RDF is orientationally averaged over the angular coordinates and much of the detail information of the local solution structure can be lost as a result of the cancellation of contributions from regions of low and high probability at the same distance but different parts of the local solution structure.[36] To overcome the limitations of RDF, the spatial distribution function (SDF) was proposed.[37] It spans both the radial and angular coordinates of the interatomic separation vector and is well suited to describe three-dimensional density distribution of molecules in a local coordinate system attached to the solute molecule or a part of it.

3. Results

In the present contribution, we focus on the analysis of MD simulated aqueous solution of dipeptide with transition metal chlorides (Mn^{2+} to Zn^{2+}). The ordering of water molecules interacting with dipeptide is specific to the local structure of solute, its stereochemistry, and the distribution of functional groups. Changes in the three-dimensional arrangement of these water molecules not only may affect the dipeptide structure but also may seem to play an important role in regulating their interactions and biological functions. The distribution of solvent near the peptide is complicated by many factors including water−water, ion−ion, ion−water, peptide−water, and peptide−ion interactions, and by coupling among those interactions. It will be instructive to summarize first the results regarding ion hydration before going to the detailed discussion of results

TABLE 3: Water Coordination Number of Metal Ions, Diffusion Coefficients, and Intermolecular Energies for Three Different Systems[a]

system	ion	CN	D_w (10^{-5}cm·s^{-2})	D_M (10^{-5}cm·s^{-2}) metal ions	ion−water intermolecular energy (kJ·mol^{-1})[b]
I	Mn	6	2.32	0.56	−2604
	Fe	6	2.32	0.5	−2736
	Co	6	2.32	0.48	−2874
	Zn	6	2.32	0.42	−2946
	Ni	6	2.29	0.42	−2993
	Cu	6	2.33	0.41	−3046
II	Mn	5.60 ± 0.1	1.97	0.43	−1850
	Fe	5.60 ± 0.1	1.95	0.42	−1997
	Co	5.60 ± 0.1	1.94	0.41	−2109
	Zn	5.80 ± 0.1	1.93	0.4	−2313
	Ni	5.80 ± 0.1	1.94	0.42	−2334
	Cu	5.98 ± 0.02	1.93	0.43	−2509
III	Mn	5.92 ± 0.05	2.18	0.48	−2487
	Fe	6	2.20	0.46	−2670
	Co	6	2.18	0.46	−2894
	Zn	6	2.19	0.47	−2951
	Ni	6	2.19	0.49	−2987
	Cu	6	2.16	0.4	−2947

[a] Experimental diffusion coefficients[58] at infinite dilution, in units 10^{-5} cm^2/s: Mn^{2+}, 0.681; Fe^{2+}, 0.715; Co^{2+}, 0.732; Ni^{2+}, 0.679; Cu^{2+}, 0.714; Zn^{2+}, 0.703; pure water, 2.25. [b] Uncertainty in energy is estimated as 10 kJ/mol.

for dipeptide. Previously, ion hydration was a subject of many experimental, theoretical, and simulation studies,[38−51] both for pure ion solutions and for ions in presence of other solute molecules.

3.1. Ion Hydration. The relevant hydration parameters such as coordination numbers, diffusion coefficients, and intermolecular energies of divalent transition metal ions (Mn to Zn) in water, evaluated from the molecular dynamics simulation of three different systems, are summarized in Table 3. In the case of system I, all the ions have hydration number 6, corresponding to the stable unperturbed octahedral hydration shell, which is also in agreement with work of Babu and Lim.[29] A notable change in the coordination number of metal atoms in system II can be observed. Higher concentration of ions leads in some cases to substitution of one of the water molecules in the hydration shell by an anion. In case of system III, the hydration number for all ions is again 6, with exception of small deviation for Mn^{2+} caused also by interference of the anion. We, however, never observed dipeptide atoms in direct contact with ions.

The ion−water interaction energy is another quantity describing hydration of ions. Generally, the lower the intermolecular energy value, the stronger is the binding between the interacting species. However, this ion−water interaction energy is not directly related to the solvation free energies, since it differs by the entropy contribution and by the change of water−water interaction energy caused by addition of the ion. The order of decreasing energy (which corresponds to stronger ion−water association) follows exactly the order of decreasing ion sizes (cf. Table 1) $Mn^{2+} > Fe^{2+} > Co^{2+} > Zn^{2+} > Ni^{2+} > Cu^{2+}$. An interesting observation is that, compared to the case of low concentration (system I), an increase of salt concentration (system II) leads to noticeably higher (less negative) interaction energies while an increase in dipeptide concentration (system III) affects the ion−water energy in different ways, leading also to violation of the order observed at low concentration. The presence of other ions, due to their strong electrostatic interactions, seems to perturb the hydration shells of divalent cations; the presence of bulky, partially hydrophobic dipeptide can make the hydration shell stronger.

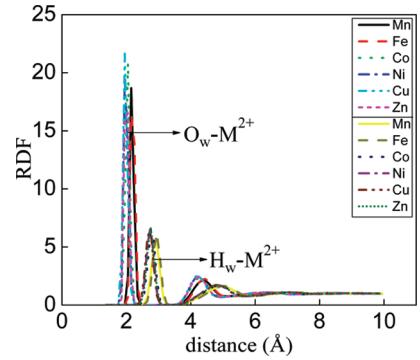

Figure 2. RDF between divalent metal ions and water oxygen and water hydrogen calculated for system I.

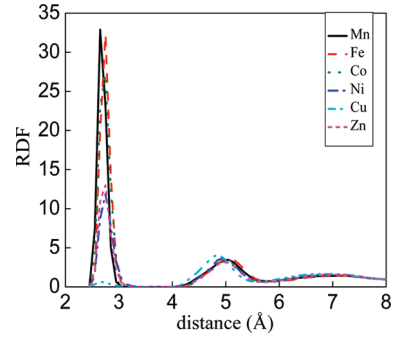

Figure 3. RDF of metal ions with chloride ions.

The RDFs of O and H atoms of water molecules and metal ions are shown in Figure 2. The divalent cations attract water oxygens electrostatically, which is manifested by distinct features in the RDF (Figure 2). All RDFs demonstrate a high first peak corresponding to water molecules in the first hydration shell, as well as well resolved second maximum. The first hydration shell consists of six water molecules for all metal ions. The structural comparison of the transition metal ions Mn^{2+}, Fe^{2+}, Co^{2+}, Ni^{2+}, Cu^{2+}, and Zn^{2+} show near similarity in the O_w-M^{2+} RDFs. The peaks of O_w-Mn^{2+} and O_w-Fe^{2+} are smaller and broader than other oxygen−metal ions located at a slightly smaller distance. The second shell also shows a well-defined maximum for all metal ions. RDFs between the first and the second peak are zero (or nearly zero in a few cases), showing the practical absence of water exchanges between the first and second coordination shells on the time scale of simulations. H_w-M^{2+} RDF in Figure 2 also shows two distinct peaks that are shifted by about 0.5 Å from the corresponding O_w-M^{2+} RDFs. Beyond the second hydration shell, the RDF structure became rather homogeneous for all ions.

Metal ion−chloride anion RDFs, computed for system II, are shown in Figure 3. They differ by the height of the first peak, corresponding to a contact ion pair. This peak is practically absent for Cu^{2+} ions, which correlate well with data from Table 3 showing that Cu^{2+} ions essentially keep hydration number 6 even in the concentrated solution. In contrast, metal ions Mn^{2+}, Fe^{2+}, and Co^{2+} have a high first RDF peak with chloride anions, and they also have the largest decrease in the hydration number, down to 5.6, which is explained by the chloride anion substituting one of water molecules in the first hydration shell.

3.2. Hydration of Polar Groups of Dipeptide. Interpretation of actual distribution of water molecules and ions around a peptide atom from the corresponding RDF can be complicated by the existence of other atoms in the peptide, or the volume exclusion effect, and the electrostatic interactions between charged peptide groups and solvent. As a rule of thumb, the

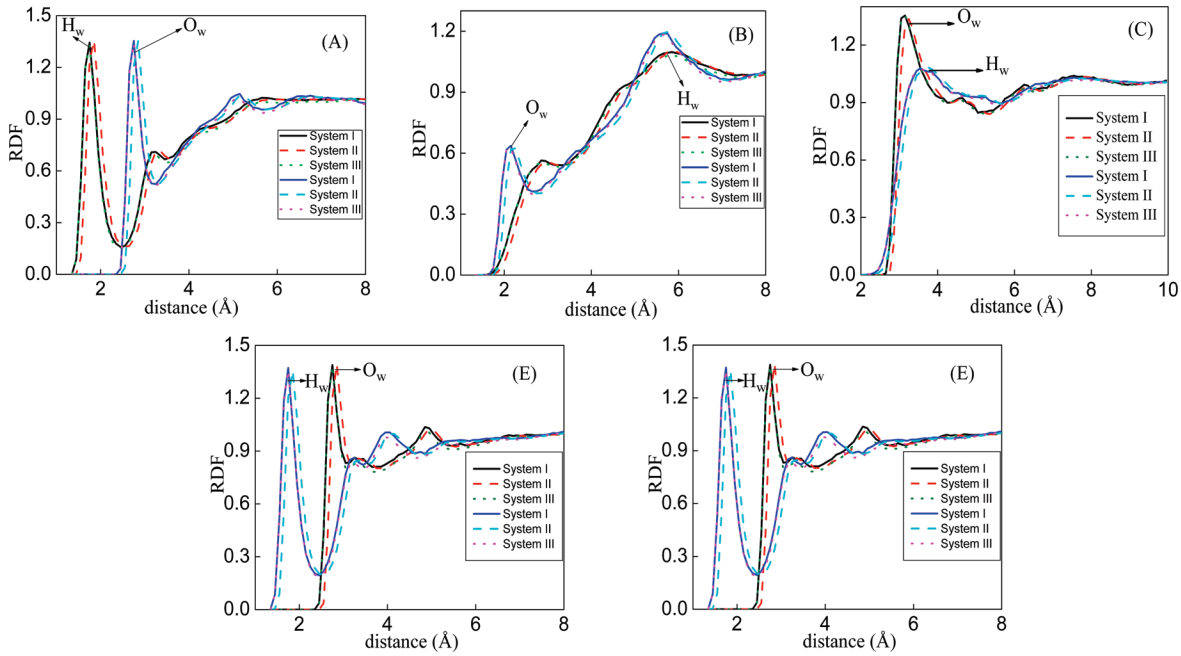

Figure 4. RDF between polar atoms of GG dipeptide and water oxygen and hydrogen computed for Mn^{2+} ion and systems I, II, and III: (A) O_p of peptide carbonyl; (B) H_p of peptide amino group; (C) N_h of NH_2; (D) O_h of hydroxyl oxygen; (E) O_c of COOH (carbonyl).

charged groups in a peptide are well exposed to solvent, while the nonpolar groups are less exposed and sterically hindered by other peptide atoms from accessing to solvent. We, therefore, selected five characteristic polar peptide atoms, H_p of the peptide NH group, O_p of the peptide C═O group, N_h of NH_2, O_h of OH (hydroxyl), and O_c of COOH (carbonyl) (the atom names are displayed in Figure 1). These RDFs, for systems I, II, and III and Mn^{2+} metal ions, are shown in Figure 4A−E.

The RDF between peptide carbonyl O_p and H_w reveals that the coordination shell is characterized by a major peak around 1.8 Å (Figure 4A). The coordination number, computed at the RDF minimum of 2.5 Å, shows on an average two hydrogen atoms in the coordination shell of this site of the peptide. The O_p-O_w distribution function approaches a maximum at a distance of 2.8 Å, again with a coordination number around 2. The second maximum of the O_p-H_w RDF at about 3.1 Å is formed by two other hydrogen atoms of the two water molecules in the first hydration shell. These distribution functions are an indication of hydrogen bonds between the acceptor of the solute and donors of water molecules; that is, the oxygen of the peptide C═O group is strongly hydrogen bonded with two water molecules. The formation and breaking of such hydrogen bonds may play an important role in determining the functionality of peptides.

The RDFs of water oxygen and hydrogen around the hydrogen of the NH group in the peptide bond are plotted in Figure 4B. In typical GG dipeptide conformations, the NH group can be partially protected from solvent access by surrounding atoms. Therefore, the distribution of water molecules around the group is relatively low. However, there is a well-defined peak of H_pO_w RDF at 1.9 Å distance, which is typical for a hydrogen bond formed by an amino group.[52] H_pH_w RDF has a first peak at a somewhat larger distance, showing that the hydrogen atoms of water are not in contact with the peptide atoms and direct outward from the group. Analysis of coordination numbers shows one water molecule bound to this site of dipeptide. Such a hydration pattern arises due to the electrostatic interaction between the water molecules and the positively charged amino group hydrogens. The H_pO_w and H_pH_w RDFs have a stronger second maximum at about 5.5 Å distance, which is a combined effect of water in the second hydration shell, as well as of water hydrating the end NH_2 and COOH groups of the dipeptide.

RDF between nitrogen of the terminal amino group NH_2 and water oxygen shows maximum at about 3 Å distance typical for a hydrogen bond donated by the amino group to water (Figure 4C). The maximum of N_h-H_w RDF is at about a 0.5 Å larger distance, indicating that both water hydrogens are directed outward from this group and located at about the same distance from the nitrogen. There is no well expressed RDF minimum indicating the absence of the well-defined hydration shell of the dipeptide terminal amino group.

RDFs between water and oxygens of the terminal COOH group of dipeptide are shown in Figure 4D,E. H_w-O_h RDF, with coordination number 1, shows one water molecule donating a hydrogen bond to the hydroxyl oxygen (Figure 4D). O_w-O_h RDF has a higher first maximum, corresponding to coordination number 2.5, which is explained by contribution of oxygen of another water molecule bound to the hydroxyl hydrogen, as well as due to other water molecules occasionally appearing near the terminal COOH group. H_w-O_c RDF (Figure 4E) shows a peak at about 2 Å distance typical for a hydrogen bond. RDFs between the O_c atom and O and H atoms of water have first peaks very similar to the corresponding peaks for the carbonyl of the peptide group (Figure 4A), showing two water molecules bound by hydrogen bonds to the carbonyl oxygen. The O_w-O_c RDF has, however, a second maximum at about 4 Å distance, which is absent in O_w-O_p RDF. This maximum comes evidently from water bound to the hydroxyl oxygen of the dipeptide.

Parts A−E of Figure 4 show that all dipeptide−water RDFs depend very little on the concentration of ions or dipeptide. The only feature one can observe is that most of dipeptide−water RDFs in the case of system II (high salt concentration) show the first RDF maximum slightly shifted out of dipeptide, in comparison to RDFs of systems I and III. The probable reason is that the strong electric field of divalent ions pulls some of water molecules out of dipeptide, resulting in a small shift of RDFs. Previously, similar changes of water−water RDFs upon

an increase of salt concentration were observed within the RISM theory.[41] An increase in depeptide concentration does not produce a noticeable effect on the water−dipeptide RDF, which is seen from comparison of RDFs corresponding to systems I and III.

3.3. Three-Dimensional Solvation Structure around Dipeptide: Spatial Distribution Functions. A more comprehensive understanding of solvation structure can be achieved from the spatial distribution function (SDFs). These functions are usually depicted in the form of three-dimensional iso-surfaces of spatial density in a coordinate system defined by a central molecule. Since the dipeptide molecule is rather flexible, changing its conformation repeatedly during the simulations, it is not possible to set a reasonable local basis for the whole molecule. Instead, we choose three important and relatively rigid fragments of dipeptide and built SDF around them. These SDF were used to rationalize the conclusions drawn from radial distribution functions.

Figure 5A shows the spatial distribution function of water oxygens and hydrogens around the central peptide fragment (C═O−N−H) at contour levels 3 and 2.5, respectively. The usual features of the tetrahedral hydrogen-bonded structure of water in the first solvation shell is a cap over hydrogen from the hydrogen-bond-accepting neighbor and another cup-shaped feature from the other side of the molecule, which is due to the hydrogen-bond-donating neighbor. These patterns are similar to those observed in studies of spatial solvation structure in pure water.[37,53] Figure 5B shows the solution structure for the water molecules around a terminal COOH group of GG at contour levels 3 and 2, respectively. The intensity of the COOH−water SDF is larger near the hydroxyl oxygen, which indicates a stronger hydrogen bond at this site than at the carbonyl site of the COOH group. Figure 5C shows the NH_2−water molecules interactions at contour levels 3 and 2.5, respectively. The two hydrogens in the NH_2 group also show greater affinities of forming hydrogen bonds with water molecules, binding one water to each hydrogen of the terminal NH_2 group.

3.4. Interaction of Dipeptide with Metal Ions. RDFs between metal ions and several polar atoms of dipeptide (peptide bond carbonyl oxygen O_p, nitrogen of terminal amino group N_h, and hydroxyl oxygen O_h) are shown in Figure 6A−C. All these RDFs are computed for system II. The length of the simulations was enough to ensure that the observed differences between these RDFs were statistically significant, which was checked by computations of RDF over simulation times 0.5−5 and 5−10 ns, which demonstrated the same trends (data not shown). Data of diffusion of the ions and water, as well as residence times (discussed in details below), also confirm that the ions have enough time to sample the space around the dipeptide molecule. One can see that overall RDF structures (positions of RDF maxima and minima) are rather similar for all the ions. However, the intensities of maxima differ substantially for different ions. It is also worth noting that the position of the maximum, about 5 Å, corresponds to binding with one intermediate water molecule, which belongs to the first hydration shell of the ion. There is no contact ion−depeptide maximum on any of the computed ion−dipeptide RDFs, including those for systems I and III (data not shown). The latter observation indicates that the hydration shell of divalent ions cannot be broken by the dipeptide on the time scale of the present simulations.

To investigate the possibility that direct binding of ions to dipeptide may be stable but not assessable in 10 ns simulations because of a high free energy barrier between the contact and

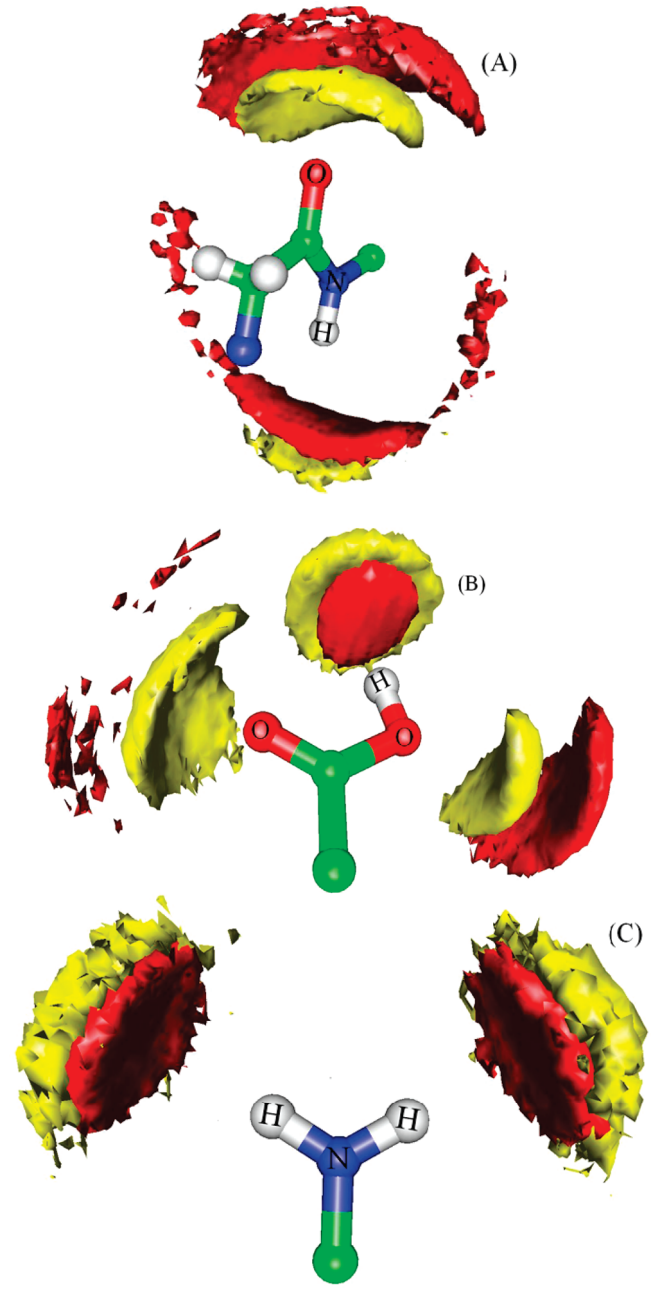

Figure 5. SDF of water oxygen and hydrogen around (A) GG central peptide group, (B) terminal COOH group, and (C) terminal NH_2 group. Calculations are done for the Mn^{2+} ion and system I. Atoms used to define SDF basis are labeled in the above figures.

solvent-separated bound states, we made a few test simulation in which an ion (Mn^{2+}, Cu^{2+}, and Zn^{2+}) was initially placed in contact with O_p oxygen of the peptide group of GG. Moreover, we put additional harmonic bond of length 2 Å and force constant 200 kJ·mol^{-1}·Å^{-2} between the ion and peptide oxygen, and kept it for 1 ns, allowing water to equilibrate properly around the ion−GG complex. Then the bond was released. In all three test simulations, we observed that the ion dissociated from GG during 1−2 ns. This test demonstrates that the contact bound state is not stable and disappears after a relatively short observation time, while we never observed the reverse process of formation of directly bound state. The instability of the directly bound state can also be rationalized from the observation that the partial charge of water oxygen is −0.82, while the charge of the carbonyl oxygen is −0.57. That is why, within the given force field, the water−ion attraction is stronger than

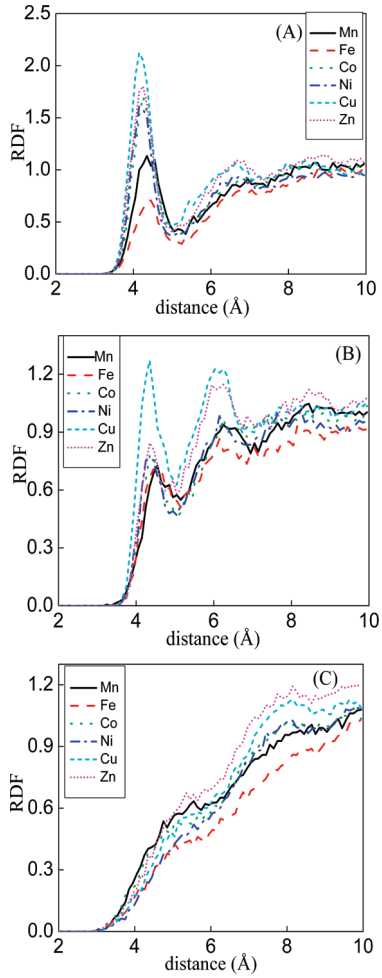

Figure 6. RDFs between metal ions and polar atoms of GG dipeptide: (A) carbonyl oxygen O_p, (B) hydroxyl oxygen O_h, and (C) N_h of NH_2 terminal group. Calculations are done for System II.

the water−carbonyl attraction, which leads to stronger ion−water binding than ion−peptide binding.

A reservation still should be made that the discussed above statement about the impossibility of the dipeptide to break the hydration shell of divalent ions is valid within the classical nonpolarizable force field model used in this work. It might be possible that the strong electric field of the divalent ion, when it is in near contact with the peptide oxygen, causes a shift of the electron density, which would lead to a more negative oxygen charge and to a stronger binding of the ion to the depeptide. Peculiarities of the electron shell of transition metals with valence d-electrons, not taken into account by simple spherically symmetric pair-additive LJ potential, may also play a role. A proper account of all these factors is, however, possible only within the quantum-chemical approach, which is out of scope of the present investigation. Here we mention that previous DFT studies[54,55] demonstrated that even negatively charged carboxylates might have barriers over 20 kcal/mol to break the first hydration shell of divalent metal ions.

Comparing RDF intensities corresponding to the solvent-mediated ion binding to GG, one can see that Fe^{2+} has the lowest intensity and indicates weaker affinity with the oxygen atoms of dipeptide. In contrast, the Cu^{2+} ions show the strongest affinity with the O_p and O_c dipeptide atoms among all considered ions. From Table 3 one can also note that Cu^{2+} is the only ion (of the considered ions) that keeps its hydration shell almost intact, even in the concentrated ion solution, which can be interpreted as Cu^{2+} having the most stable hydration shell. Water molecules bound to Cu^{2+}, have hydrogen atoms directed out of the ion. One of these hydrogens can form a hydrogen bond to the carbonyl oxygen of dipeptide, building the configuration C═O−H_w−O_w−cation. Other ions bind to the carbonyl oxygen of dipeptide according to the same scheme, but their binding is weaker. Computation of coordination numbers for O_p−M^{2+} RDF yields the following sequence: 0.117, 0.106, 0.10, 0.094, 0.089, and 0.05 for Cu^{2+}, Zn^{2+}, Co^{2+}, Ni^{2+}, Mn^{2+}, and Fe^{2+}, respectively. One can speculate that for water in the first coordination shell of Cu^{2+}, it might be easier to form a hydrogen bond to the carbonyl oxygen of dipeptide than to other water molecules. Other ions are larger and have a more relaxed first hydration shell, so that first shell water molecules may more easily form hydrogen bonds with other water molecules of the second hydration shell, compared to the case for the dipeptide oxygen.

In Figure 6B, showing RDFs between metal ions and hydroxyl oxygen of GG, Cu^{2+} ions have again the strongest peak intensity in comparison with other metal ions. The peak is, however, somewhat lower than the corresponding peak in the Cu^{2+}−O_p RDF. All M^{2+}−O_c RDFs also show a second maximum at about 6 Å distance, which in fact corresponds to ions bound to the peptide carbonyl oxygen O_p. The divalent cations are electrostatically repelled from the peptide NH_2 group and do not have any distinct feature in the RDFs (Figure 6C). Still, one can note a fairly higher preference of Zn^{2+} ions to this group of dipeptide and a lower preference for the Fe^{2+} ion. Comparing different ion−dipeptide RDFs, one can note a general trend that smaller ions (Cu^{2+}, Zn^{2+}) bind to dipeptide stronger than larger ones (Fe^{2+}, Mn^{2+}). The connection is, however, not strict. The degree of binding is a result of a very delicate balance between many competing interactions (ion−water, water−water, water−dipeptide, and dipeptide−ion), which is why it may be strongly affected by small changes in the ion interaction parameters.

3.5. Ion, Water, and Peptide Dynamics. The diffusion coefficient provides a link between the hydration and mobility of an ion. The magnitude of variation of the diffusion coefficient of water in the presence of different metal salts is very little within each of systems I, II, and III (see Table 3). Experimental data[56] (given in the footnote to Table 3) also show very similar diffusion coefficients for this set of ions. On the other hand, the diffusion coefficient becomes noticeably smaller with an increase in concentration. By comparing results of system II and system III, one can conclude that salt retards diffusion of water to a larger degree than the dipeptide. Diffusion coefficients of ions depend rather little on both their type and concentration. Mostly, one can note somewhat faster diffusion of larger ions (Mn, Fe, Co) in system I (low concentration). The results can be understood by imaging a picture of ions moving together with their hydration shell, which explains both the weak dependence of diffusion on the ion type and the decrease of water diffusion with the ion concentration.

Diffusion coefficients reflect in some sense the "average" motion of a certain type of molecules. Another important aspect of dynamics in liquids is residence times (or life times) of different associated states, such as hydrogen bonds, coordination in a first or in a second hydration shell, etc. We have investigated residence times of water molecules and ions around possible binding sites of the dipeptide. We use the definition of residence time introduced by Impey et al.[57] and later used for studies of water dynamics in the hydration shells of ions,[58] which we describe briefly here for the convenience of the reader. We define distance r_{hyd} corresponding to the border of the hydration

TABLE 4: Residence Times for Some Bound States[a]

sites	r_{hyd}/Å	residence time/ps
Water−Dipeptide, System I with Mn^{2+}		
O_w-O_p	3.2	4.7
O_w-O_c	3.2	4.3
O_w-O_h	3.2	4.1
O_w-H_p	2.6	3.7
O_w-N_h	4.3	6.6
Water−Dipeptide, System II with Mn^{2+}		
O_w-O_p	3.3	4.9
O_w-O_c	3.3	5.0
O_w-O_h	3.3	4.6
O_w-H_p	2.7	3.8
O_w-N_h	4.3	6.8
estimated uncertainty	0.1	0.2
Ion−Dipeptide, System II		
$Mn^{2+}-O_p$	5.3	13.7
$Fe^{2+}-O_p$	5.2	11.2
$Co^{2+}-O_p$	5.1	17.2
$Zn^{2+}-O_p$	5.0	18.2
$Ni^{2+}-O_p$	4.9	16.2
$Cu^{2+}-O_p$	4.9	20.0
estimated uncertainty	0.1	2.0

[a] r_{hyd} is determined as the first minimum of the corresponding RDF.

shell (or distance defining a bound state) as the first minimum of the corresponding RDF. We begin to count the lifetime of a bound state when the two sites occur at a distance less than r_{hyd} and finish when the two sites go apart, so that the distance between them again occurs larger than r_{hyd}. Exits from the hydration shell that are shorter than 2 ps are not accounted for to ignore cases when a molecule leaves the coordination shell only temporarily without properly entering the bulk solution. From these events, the probability for a molecule that just entered the hydration shell to remain there during time t is calculated, and the final average residence time is defined from the exponential decay of this probability. In the case when the statistics of entries and exits from the hydration shell is too poor to build the probability distribution over time, a simple average of the observed residence times is used. We used the later definition in calculations of residence times of ions near dipeptide.

The collected residence times for water and ions around different sites of the GG dipeptide are given in Table 4. The residence time of water around the polar atoms of GG is in the range 4−6 ps, which is typical for hydrogen bonds in pure water (defined as 4.5 ps for pure water within the same water model[58]). One can see that in system II the residence times become somewhat longer, which is consistent with the overall slowing down of dynamics upon increase of salt concentration. The residence time of ions near the peptide oxygen is on the order of 10−20 ps. One can notice that the ions with a higher ion−GG RDF maximum (Figure 6A) have also a longer residence time, indicating their stronger binding to GG. Both RDF and residence times provide the following order of the binding strength: $Fe^{2+} < Mn^{2+} < Ni^{2+} < Co^{2+} < Zn^{2+} < Cu^{2+}$. It is remarkable that this order does not follow the order of ion sizes and ion−water interaction energies discussed in section 3.1: Mn^{2+} and Ni^{2+} ions take now other places. Ion−dipeptide interaction is a complex phenomena resulting from a delicate balance of ion−water, dipeptide−water, and ion−depeptide interactions, modulated additionally by specific features of 3-dimensional coordination of water molecules in the hydrated shells of ions and dipeptide. One can also draw analogues with unusual properties of the Li^+ ion among other alkali ions, where it shows properties somewhere between K^+ and Cs^+ ions in the effect on hydrophobic interactions[26] and in the order of binding affinities of alkali ions to DNA.[59] This work shows another example that the binding affinity of divalent ions does not necessary follow the order of ion sizes.

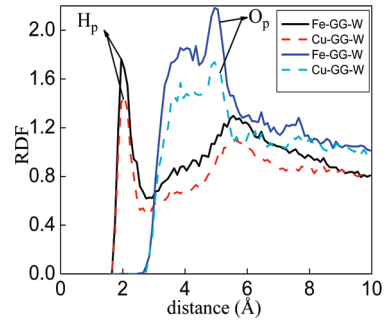

Figure 7. RDF showing interactions between peptides: O_p-H_p and O_p-O_p, in solutions with metal ions Fe and Cu (system III).

Besides important information on the dynamics of water and ions around the dipeptide, the calculated diffusion coefficient and residence times show that our simulations are well equilibrated and sampling from 10 ns dynamics is sufficient to describe properties of this system. Diffusion coefficients of glycylglycine in the Mn^{2+} salt solution for systems I, II, and III are 0.74, 0.38, and 0.52 (multiplied by 10^{-5} $cm^2 \cdot s^{-1}$), respectively. The diffusion of order 10^{-5} $cm^2 \cdot s^{-1}$ means that the molecules travel on average ~20 Å in 1 ns, which allows them to travel across the simulation box during the time of simulations. Residence times on the order of a few tens of picoseconds mean that the molecules never get stacked in some tightly bound states. The only exception is ion−water interactions. In most of the cases, we did not register any exchanges of water molecules in the first coordination shell of metal ions with the molecules in the bulk (these cases correspond to the exact coordination number 6 in Table 3). In other cases, only a few exchanges were registered during the simulation. A slow exchange of water molecules in the first coordination shell of divalent ions, which may be on the order of microseconds, is a known phenomenon.[60,61] This slow process, however, does not affect sampling of water−dipeptide and ion−dipeptide interactions. An eventual exchange of water molecules in the first hydration shell of an ion leads to practically the same state as if such transition did not occur, since all water molecules are identical.

3.6. Dipeptide−Dipeptide Interactions. Water- and ion-mediated interaction between peptides is ultimately responsible for the process of protein folding. In this respect, two types of interactions are of primary importance: hydrogen bonds between carbonyl C═O and amino group N−H of the peptide backbone (responsible for formation of α-helixes and β-sheets in proteins), and the hydrophobic interaction. For GG dipeptide, studied in this work, hydrophobic interactions may be of less importance, and we have studied formation of peptide hydrogen bond and the effect of ions on it.

The RDFs between carbonyl oxygen of one dipeptide and amide hydrogen of another dipeptide, computed for system III, exhibit a weak tendency for pairing by forming intermolecular hydrogen bonds (Figure 7). H_p-O_p RDF has a characteristic peak at 2 Å corresponding to a hydrogen bond. Integration over the first RDF peak yields coordination numbers 0.028 and 0.022 for Fe^{2+} and Cu^{2+} ions, respectively, showing low (2−3%) probability of formation of such pairs at a given dipeptide

concentration. The O_p-O_p RDF does not have, however, a clear first maximum. In the snapshots, one can see that stacking of one peptide carbonyl by another peptide carbonyl may take place. For this reason, another RDF maximum is observed at a longer distance of 5 Å. Generally, peptide−peptide RDFs do not show strong association of peptide molecules, they remain essentially dissolved in water. This is also confirmed by observation of snapshots (data not shown) where one can only occasionally observe formation of dipeptide pairs. Such a behavior is also in agreement with experiment, showing the solubility of the GG dipeptide as 1.74 M,[62] which is higher than our dipeptide concentration in system III (0.5 M).

4. Discussion

Studies on the solvation structure and dynamics in aqueous solutions of dipeptides and transition metal salts have been carried out. The complicated effects involving interactions among peptide, water, and ions have been interpreted in a consistent manner using various RDFs and SDFs. While RDFs provide accurate quantitative comparison of hydration properties of ions and the dipeptide at different compositions of the system, as well as typical distances between the atoms and coordination numbers, SDF provides overall a 3-dimensional view of the hydration structure, complementing conclusions drawn from radial distribution functions. Also, diffusion coefficients and various residence times of water and ions around the depeptide have been determined, which provide important information about the dynamics of molecules in this system.

The analysis of results, given in detail in the previous sections, shows that divalent ions and dipeptide molecules, being dissolved in aqueous solution, do not affect each other much. In most of cases, divalent ions keep their hydration shell consisting of six water molecules, which can be broken only by Cl^- anions at high salt concentrations, and interact with the dipeptide mostly as $Me^{2+}-6H_2O$ complexes. The simulations show the presence of a well-defined first hydration shell around the dipeptide, with water molecules forming hydrogen bonds to the polar groups of the dipeptide. The exchange of water molecules in the first hydration shell of the dipeptide with water in the bulk occurs on a few picoseconds time scale. The water solvation structure around dipeptides remains mostly unaffected by ions. Ions never interact with the dipeptide directly, but only though an intermediate water molecule. Nevertheless, the presence of divalent metal ions leads to a number of noticeable effects. The strong electric field of divalent metal ions causes a shift in the dipeptide−water RDFs at higher ion concentrations. Higher salt concentrations lead also to increased residence times and slower diffusion rates.

The affinity of ions for the dipeptide molecule depends on the type of ion, following the order $Cu^{2+} > Zn^{2+} > Co^{2+} > Ni^{2+} > Mn^{2+} > Fe^{2+}$. In general, smaller ions (Cu^{2+}, Zn^{2+}) demonstrate stronger binding to the dipeptide than the larger ones (Fe^{2+}, Mn^{2+}); however, the affinity order does not follow the size order exactly. Ions with higher affinity demonstrate also a longer residence time of binding to the dipeptide. The residence times of ion−dipeptide association are, however, rather short (10−20 ps) demonstrating the fast dynamical character of dipeptide−hydrated ion interactions. Simulations do not show any stronger association of peptide molecules, indicating their dissolution in water. It follows from this study that the qualitative effects of mixed ion−depeptide aqueous solutions can be well understood from examining the behavior of salt and dipeptide in aqueous solutions taken separately. The above results may be of potential interest to future researchers on these molecular interactions.

The simulations of this paper were carried out within a rather simple force field including only Lennard-Jones and electrostatic terms for intermolecular interactions. Accurate treatment of the electron structure of transition metals may lead to a more complicated functional form of the ion−water interaction potentials, including three-order and higher terms, polarization, etc.[20,43,44] It seems, however, plausible, that due to the strong electric field of divalent cations, the water molecules in the first hydration shell will be in any case strongly bound to the cation, resulting in the overall ion hydration structure similar to that obtained within the simple model, and producing results qualitatively similar to results obtained in the present work.

Acknowledgment. M.S.S. thanks the Swedish Institute for awarding a guest scholarship and Department of Materials and Environmental Chemistry, Stockholm University, for providing suitable facilities to carry out this work. Computer facilities have been granted by the Swedish National Infrastructure for Computing (SNIC).

References and Notes

(1) Von Hippel, P. H.; Schleich, T. *Acc. Chem. Res.* **1969**, *2*, 257–265.
(2) Jencks, W. P. *Catalysis in Chemistry and Enzymology*; McGraw-Hill: New York, NY, U.S., 1969; p 351.
(3) Perutz, M. F. *Science* **1978**, *201*, 1187–1191.
(4) Von Hippel, P. H.; Schleich, T. *Structure and Stability of Biological Macromolecules*; Timasheff, S. N., Fasman, G. D., Eds.; Marcel Dekker: New York, NY, U.S., 1969; pp 417−573.
(5) Collins, K. D.; Washabaugh, M. W. *Q. Rev. Biophys.* **1985**, *18*, 323–422.
(6) Baldwin, R. L. *Biophys. J.* **1996**, *71*, 2056–2063.
(7) Dill, K. A. *Biochemistry* **1990**, *29*, 7133–7155.
(8) Israelachvili, J.; Wennerström, H. *Nature* **1996**, *379*, 219–225.
(9) Berg, J. M. *Annu. Rev. Biophys. Biophys. Chem.* **1990**, *19*, 405–421.
(10) Stryer, L. *Biochemistry*, 4th ed.; W. H. Freeman and Co.: New York, NY, U.S., 1995.
(11) Lipscomb, W. N.; Strater, N. *Chem. Rev.* **1996**, *96*, 2375–2433.
(12) Holm, R. H.; Kennepohl, P.; Solomon, E. I. *Chem. Rev.* **1996**, *96*, 2239–2314.
(13) Christianson, D. *Prog. Biophys. Mol. Biol.* **1997**, *67*, 217–252.
(14) Lippard, S. J.; Berg, J. M. *Principles of Bioinorganic Chemistry*; University Science Books: Mill Valley, CA, U.S., 1994.
(15) Cappa, C. D.; Smith, J. D.; Messer, B. M.; Cohen, R. C.; Saykally, R. J. *J. Phys. Chem. B* **2006**, *110*, 5301–5309.
(16) Näslund, L. Å.; Edwards, D. C.; Wernet, P.; Bergmann, U.; Ogasawara, H.; Pettersson, L. G. M.; Myneni, S.; Nilsson, A. *J. Phys. Chem. A* **2005**, *109*, 5995–6002.
(17) Omta, A. W.; Kropman, M. F.; Woutersen, S.; Bakker, H. J. *Science* **2003**, *301*, 347–349.
(18) Leberman, R.; Soper, A. K. *Nature* **1995**, *378*, 364–366.
(19) Petersen, P. B.; Saykally, R. J. *J. Phys. Chem. B* **2006**, *110*, 14060–14073.
(20) Rode, B. M.; Schwenk, C. F.; Tongraar, A. *J. Mol. Liq.* **2004**, *110*, 105–122.
(21) Perkyns, J. S.; Wang, Y.; Pettitt, B. M. *J. Am. Chem. Soc.* **1996**, *118*, 1164–1172.
(22) Kohtani, M.; Jarrold, M. F.; Wee, S.; O'Hair, R. A. J. *J. Phys. Chem. B* **2004**, *108*, 6093–6097.
(23) Imai, T.; Kinoshita, M.; Hirata, F. *Bull. Chem. Soc. Jpn.* **2000**, *73*, 1113–1122.
(24) Wong, C. H. S.; Ma, N. L.; Tsang, C. W. *Chem.−Eur. J.* **2002**, *8*, 4909–4918.
(25) Dzubiella, J. *J. Am. Chem. Soc.* **2008**, *130*, 14000–14007.
(26) Thomas, A. S.; Elcock, A. H. *J. Am. Chem. Soc.* **2007**, *129*, 14887–14898.
(27) Cornell, W. D.; Cieplak, P.; Bayly, C. I.; Gould, I. R.; Merz, K. M.; Ferguson, D. M.; Spellmeyer, D. C.; Fox, T.; Caldwell, J. W.; Kollman, P. *J. Am. Chem. Soc.* **1995**, *117*, 5179–5197.
(28) Toukan, K.; Rahman, A. *Phys. Rev. B* **1985**, *31*, 2643–2648.
(29) Babu, C. S.; Lim, C. *J. Phys. Chem. A* **2006**, *110*, 691–699.
(30) Heinzinger, K. *Physica* **1985**, *131B*, 196–216.
(31) Lyubartsev, A. P.; Laaksonen, A. *Comput. Phys. Commun.* **2000**, *128*, 565−589 (see also http://www.mmk.su.se/mdynamix).
(32) Tuckerman, M.; Berne, B. J.; Martyna, G. J. *J. Chem. Phys.* **1992**, *97*, 1990–2001.

(33) Ewald, P. P. *Ann. Phys.* **1921**, *64*, 253–287.
(34) Melchionna, S.; Ciccotti, G.; Holian, B. L. *Mol. Phys.* **1993**, *78*, 533–544.
(35) Allen, M. P.; Tildesley, D. J. *Computer Simulation of Liquids*; Clarendon Press: Oxford, U.K., 1987.
(36) Laaksonen, A.; Kusalik, P. G.; Svishchev, I. M. *J. Phys. Chem. A* **1997**, *101*, 5910–5918.
(37) Kusalik, P. G.; Svishchev, I. M. *Science* **1994**, *265*, 1219–1221.
(38) Kinoshita, M.; Hirata, F. *J. Chem. Phys.* **1997**, *106*, 5202–5215.
(39) Chong, S. H.; Hirata, F. *J. Phys. Chem. B* **1997**, *101*, 3209–3220.
(40) Hirata, F. *Bull. Chem. Soc. Jpn.* **1998**, *71*, 1483–1499.
(41) Pettitt, B. M.; Rossky, P. J. *J. Chem. Phys.* **1986**, *84*, 5836–5844.
(42) Dang, L. X.; Pettitt, B. M. *J. Am. Chem. Soc.* **1987**, *109*, 5531–5532.
(43) Floris, F.; Persico, M.; Tani, A.; Tomasi, J. *Chem. Phys.* **1995**, *195*, 207–220.
(44) Spångberg, D.; Hermansson, H. *J. Chem. Phys.* **2004**, *120*, 4829–4843.
(45) Dang, L. X.; Pettitt, B. M. *J. Chem. Phys.* **1987**, *86*, 6560–6561.
(46) Guardia, E.; Rey, R.; Padro, J. A. *J. Chem. Phys.* **1991**, *155*, 187–195.
(47) Chitra, R.; Smith, P. E. *J. Phys. Chem. B* **2000**, *104*, 5854–5864.
(48) Inada, Y.; Mohammed, A. M.; Loeffler, H. H.; Funahashi, S. *Helv. Chim. Acta* **2005**, *88*, 461–469.
(49) Krekeler, C.; Delle Site, L. *J. Phys.: Condens. Matter* **2007**, *19*, 192101.
(50) Ikeda, T.; Boero, M.; Terakura, K. *J. Chem. Phys.* **2007**, *127*, 074503.
(51) Xu, M.; Larentzos, J. P.; Roshdy, M.; Criscenti, L. J.; Allen, H. C. *Phys. Chem. Chem. Phys.* **2008**, *10*, 4793–4801.
(52) Scheiner, S. *J. Phys. Chem. B* **2005**, *109*, 16132–16141.
(53) Jalili, S.; Akhavan, M. *J. Comput. Chem.* **2010**, *31*, 286–294.
(54) Dudev, T.; Lin, Y. L.; Dudev, M.; Lim, C. *J. Am. Chem. Soc.* **2003**, *125*, 3168–3180.
(55) Babu, C. S.; Lim, C. *J. Am. Chem. Soc.* **2010**, *132*, 6290–6291.
(56) Mills, R.; Lobo, V. M. M. *Self-diffusion in electrolyte solutions: A critical examination of data compiled from the literature*; Elsevier: Amsterdam, The Netherlands, 1989.
(57) Impey, R. W.; Madden, P. A.; McDonald, I. R. *J. Phys. Chem.* **1983**, *87*, 5071–5083.
(58) Lyubartsev, A. P.; Laaksonen, A. *J. Phys. Chem.* **1996**, *100*, 16410–16418.
(59) Lyubartsev, A. P.; Laaksonen, A. *J. Chem. Phys.* **1999**, *111*, 11207–11215.
(60) Draper, D. E.; Grilley, D.; Soto, A. M. *Annu. Rev. Biophys. Biomol. Struct.* **2005**, *34*, 221–243.
(61) Egorov, A. V.; Komolkin, A. V.; Lyubartsev, A. P.; Laaksonen, A. *Theor. Chem. Acc.* **2006**, *115*, 170–176.
(62) Breil, M. P.; Mollerup, J. M.; Rudolph, E. S. J.; Ottens, M.; van der Wielen, L. A. M. *Fluid Phase Equilib.* **2004**, *215*, 221–225.

JP108376J